Accepted: 22 March 2018

DOI: 10.1111/fwb.13114

ORIGINAL ARTICLE

WILEY Freshwater Biology

Characterisation and reactivity continuum of dissolved organic matter in forested headwater catchments of Andean Patagonia

Roberto Daniel Garcia | **María del Carmen Diéguez** | **Marina Gerea** | **Patricia Elizabeth Garcia** | **Mariana Reissig**

Grupo de Ecología de Sistemas Acuáticos a escala de Paisaje (GESAP), Instituto de Investigaciones en Biodiversidad y Medioambiente (INIBIOMA, CONICET-UNComahue), San Carlos de Bariloche, Argentina

Correspondence
Roberto Daniel Garcia, Grupo de Ecología de Sistemas Acuáticos a escala de Paisaje (GESAP), Instituto de Investigaciones en Biodiversidad y Medioambiente (INIBIOMA, CONICET-UNComahue), San Carlos de Bariloche, Argentina.
Email: garciarobertodaniel@gmail.com

Funding information
Consejo Nacional de Investigaciones Científicas y Técnicas, Grant/Award Number: PIP 2011-0064; Agencia Nacional de Promoción Científica y Tecnológica, Grant/Award Number: PICT 2013-1384, PICT 2015-0066, PICT 2015-3496, PICT 2016-0499

Abstract

1. Terrestrial inputs of dissolved organic matter (DOM) make a significant contribution to the carbon pool of headwaters and the reactivity of this pool depends on its source and diagenetic state, being influenced by photochemical and biological processes. The main goal of this study was to characterise the composition and reactivity of soil and leaf litter DOM from a native forest of *Nothofagus pumilio* (Nothofagaceae), and from natural stream water, evaluating the effect of degradation processes.
2. Photo- and biodegradation laboratory experiments were conducted using DOM leached from soil and leaf litter, while the impact of photodegradation alone was also analysed through laboratory assays using stream water. The effects of photo- and biodegradation were evaluated through changes in the concentration of dissolved organic and inorganic carbon (DOC and DIC, respectively) and optical DOM proxies (absorbance and fluorescence).
3. In the initial characterisation, DOM from soil and water leachates showed naturally high humification, aromaticity and lignin content compared with the DOM of leaf litter leachate rich in non-humic compounds.
4. Photo- and biodegradation increased humification of the DOM. DOM from leaf litter leachate was more bioavailable than DOM from soil leachate, as reflected by the higher growth of bacteria, DOC consumption and DIC production. In general, biodegradation increased DOM molecular weight, aromaticity and lignin content. Changes in fluorescent DOM (FDOM) showed a trend characterised by the loss of labile protein-like compounds and an increase in refractory humic-like components.
5. Long-rod shaped bacteria were more abundant in leaf litter leachate, suggesting their preference for labile DOM, whereas cocci dominated in the humic and more biorecalcitrant DOM from soil leachate.
6. This study showed a continuum of DOM humification, with decreasing DOM reactivity from leaf litter leachate towards soil leachate and stream water. Soil leachate DOM was probably the main source of stream water DOM, as reflected by their similar signatures and close positioning in the reactivity continuum, although carbon mineralisation was much lower in soil leachate than stream water.

KEYWORDS
allochthonous dissolved organic matter, Andean catchment, biodegradation, optical proxies, photodegradation

1 | INTRODUCTION

Dissolved organic matter (DOM) comprises dissolved and colloidal compounds containing substances of low molecular weight and macromolecules (i.e., fulvic and humic compounds), constituting the largest pool of carbon on Earth (Aufdenkampe et al., 2011; Battin et al., 2009). The DOM pool includes compounds derived from terrestrial vegetation and soils, aquatic plants and phytoplankton, as well as synthetic substances. DOM can vary over space and time depending on its source, transport and environmental processing, presenting a wide range of reactivity and ecological functions (Aiken, 2014; Jaffé et al., 2008).

The dynamics of DOM in aquatic systems are complex, involving terrestrial inputs (allochthonous) and the contribution of aquatic production (autochthonous) (Battin et al., 2009; Fasching, Ulseth, Schelker, Steniczka, & Battin, 2016). Dissolved organic carbon (DOC, a proxy for DOM) plays a part in many physical, chemical and biological processes, acting as a natural sunlight attenuator and pH buffer and influencing the transport and fate of nutrients, metals and pollutants (Aiken, 2014; Michel, Matzner, Dignac, & Kögel-Knabner, 2006; Wetzel, 2001). Moreover, since DOC is the main carbon substrate for heterotrophic bacteria, it plays a key role in the dynamics of microbial communities, thereby impacting aquatic food webs (Cole et al., 2007; Guillemette & del Giorgio, 2012).

Headwaters are closely connected to the terrestrial ecosystem. Headwaters receive, transform and export downstream large amounts of allochthonous DOM, thus generating a connection between terrestrial and aquatic pathways in the carbon cycle. This biogeochemical linkage is determined by soil and vegetation features and regulated by hydrology, which in turn is governed by climate (Fasching et al., 2016; Li et al., 2016; Sobczak & Raymond, 2015). The DOM in surface water is derived largely from organic substances leached from litter and soils (Battin et al., 2009; Cole et al., 2007).

Photodegradation and biodegradation are the most important processes acting in the transformation and mineralisation of DOM (Hansen et al., 2016). Photodegradation is a chemically selective process, effective in breaking down large, aromatic molecules that absorb light in the ultraviolet region (190–380 nm) (Benner & Kaiser, 2011; Helms et al., 2008, 2014). Nevertheless, small molecules and proteinaceous DOM can also be susceptible to photochemical reactions (Chen & Jaffé, 2016; Stedmon & Cory, 2014). Heterotrophic bacteria preferentially consume carbohydrates and proteins (Benner & Kaiser, 2011) and produce humic-like compounds that contribute to the formation of stable organic carbon in soils (Kalbitz, Schmerwitz, Schwesig, & Matzner, 2003) and aquatic systems (Ishii & Boyer, 2012; Stedmon & Cory, 2014).

Low order streams of northwestern Andean Patagonia are cold-water, carbon- and nutrient-limited systems that originate in mountain lakes and/or collect snowmelt and precipitation water (Garcia, Reissig, Queimaliños, Garcia, & Diéguez, 2015). In Andean Patagonian catchments, the deciduous tree *Nothofagus pumilio* is the dominant species surrounding the headwaters at high altitudes, from 900 to 1,600 m a.s.l. (Daniels & Veblen, 2004). During the austral autumn, *N. pumilio* stands deliver massive pulses of leaf litter to soils and riparian areas, supplying low order streams above 900 m elevation with up to 26 times more detritus than other riparian shrubs (Albariño, Díaz Villanueva, & Buria, 2009; Villalba, Boninsegna, Veblen, Schmelter, & Rubulis, 1997). In the autumn, the high-water table of the Patagonian Andes increases surface run-off, thereby enhancing the transport of allochthonous materials towards streams. This leads to a rapid increase in suspended load, nutrients and DOC, while snowmelt has a more gradual influence (Garcia, Reissig, et al., 2015; Queimaliños et al., 2012). Terrestrial DOM inputs to aquatic systems of Andean Patagonia are thus shaped by highly fluctuating hydrology (Queimaliños et al., 2012) due to the seasonal precipitation and temperature pattern (autumn–winter) (Paruelo, Beltrán, Jobággy, Sala, & Golluscio, 1998). Moreover, high solar radiation with enhanced ultraviolet (UV) levels acts overall as a strong environmental agent that transforms aquatic DOM (Queimaliños et al., 2012; Zagarese et al., 2017). In fact, the optical properties of aquatic DOM accurately reflect allochthonous inputs in autumn and spring and also the effect of photochemical and biological degradation during spring and summer (Soto Cárdenas et al., 2017).

Temperate regions in South America are currently experiencing the impact of a changing climate (Garreaud, Lopez, Minvielle, & Rojas, 2013; Intergovernmental Panel on Climate Change, 2013). Patagonia is undergoing subtle but sustained warming and drying, causing an overall climate shift from cool-wet to warm-dry conditions and significant hydroclimatic (Garreaud et al., 2013; Masiokas et al., 2008) and biotic changes (Daniels & Veblen, 2004). The native *Nothofagus* (austral beech) forest treeline elevation appears to reflect this more continental-like climate and longer snow-free growing season, particularly in the northeastern Andean sector (Daniels & Veblen, 2004). If this hydroclimatic trend is sustained, it will be critical for the Andean forest treeline, affecting the C contribution from *N. pumilio* forest to soils and headwaters, and the internal processes controlling DOM transformation.

This investigation aims to characterise the composition and reactivity of DOM leached from the leaf litter and soil of a *N. pumilio* forest stand and from natural water from an adjacent low order stream of Andean Patagonia. We also aim to evaluate the processes involved in DOM transformation, and for this purpose, we performed photo- and biodegradation experiments. We characterised the DOM through analysis of chromophoric dissolved organic matter (CDOM) and its fluorescent fraction (FDOM), which provides insight into its nature and diagenetic state (Aiken, 2014), accurately tracking the impact of photo- and biodegradation processes (Chen & Jaffé, 2016; Cory & Kaplan, 2012; Fellman, Petrone, & Grierson, 2013). We hypothesised that allochthonous DOM, leached from soil and leaf litter, makes a major contribution to stream DOM, which shares optical prints with these sources, also reflecting their photochemical and biological transformation. DOM reactivity to photo- and biodegradation is expected to decrease from leaf litter towards soil

and stream water, concomitant with increasing carbon mineralisation.

2 | METHODS

2.1 | Sampling and conditioning of DOM from source material

Soil and leaf litter from native Andean Patagonian forest were obtained from a plot in the riparian zone of a low order stream (41°10′30.5″S, 71°33′19.0″W, 1,246 m elevation) within the catchment of lake Moreno East (Nahuel Huapi National Park, northwestern Patagonia). This area is characterised by soils with deposits of volcanic and pyroclastic products, high-water retention (Andisols) and forest cover of the deciduous broadleaf *N. pumilio* (Albariño et al., 2009; Garcia, Reissig, et al., 2015).

Soil samples were collected from a plot down to a depth of 3 cm, and *N. pumilio* leaves were cut directly from the trees (ca. 1.5 m) just before leaf drop (austral autumn). Samples were placed in plastic bags and stored in a cooler. In the laboratory, the soil samples were sieved (1-mm mesh) to remove coarse materials and stored at −8°C. Leaf litter was air-dried for 10 days at room temperature (~20 °C) and preserved until the start of the experiments. Although freezing and drying may affect leaching (Cuss & Guéguen, 2013), these processes resemble the natural conditions experienced by high altitude *N. pumilio* forests in the North Patagonian Andes. Moreover, it has been found that the freezing and thawing of soil do not have a strong effect on microbial biomass or community structure (Haei et al., 2011; Koponen et al., 2006).

Water samples were collected in July 2015 (austral winter) close to the outlet of a low order stream that flows into Lake Moreno, using a polycarbonate carboy (5 L; acid-washed). They were transported to the laboratory in darkness and thermally insulated. Stream water was sterilised by filtration (Millipore PVDF, 0.22 μm pore size membranes, Brazil) and used immediately for the photodegradation experiment. This stream has been characterised as ultraoligotrophic, with low nutrient (total phosphorus = 5–50 μg/L; total nitrogen = 200–500 μg/L) and DOC concentrations (0.5–3.0 mg/L), low conductivity (40–70 μS/cm^2), circumneutral pH (6.4–7.8) and high levels of dissolved oxygen (8–12 mg/L) (Garcia, Reissig, et al., 2015).

2.2 | DOM leachates

DOM leachates were obtained simultaneously from leaf and soil samples incubated separately in Milli-Q water. The soil and leaf litter samples were first dried at room temperature (~20°C) to constant weight. Subsamples of material, of 12.5 g dry weight, were placed in acid-washed and pre-combusted glass flasks with 2.5 L of sterile Milli-Q water in triplicate. The replicates were incubated inside an environmental test chamber (Sanyo MLR5, Japan) in darkness, at 10°C (mean stream water temperature during autumn) for 48 hr. Once incubation was complete, the leachates were filtered through pre-combusted glass fibre filters (Munktell MF/F, 0.7 μm pore size filters, Sweden) to obtain the DOM and the associated microbiota (heterotrophic bacteria <0.7 μm) for the biodegradation experiment. For the photodegradation experiment, the leachates were sterilised by filtration (Millipore PVDF, 0.22 μm pore size membranes).

2.3 | Water analysis

Water conductivity and pH were measured with sondes YSI 85 and Hanna HI98150 (USA), respectively.

Characterisation of DOM concentration and quality was performed in sterile-filtered (PVDF, Millipore; 0.22 μm) water samples. Dissolved organic and inorganic carbon concentrations (DOC and DIC, respectively) were measured in a carbon analyser (Shimadzu TOC-L, USA). Optical characterisation of CDOM and FDOM was carried out using UV–visible and fluorescence spectroscopy, respectively. The absorbance spectra (200–800 nm) from filtered water samples were obtained at 1-nm intervals in a UV–visible spectrophotometer (Shimadzu UV1800, USA), using a 100-mm quartz cuvette. Sterile Milli-Q water was used as reference blank to subtract from each sample spectrum. The averaged UV–visible absorbance between 700 and 800 nm was subtracted from each spectrum to correct for any offsets due to instrument baseline effects (Helms et al., 2008). The FDOM analysis was performed by scanning the water samples in a spectrofluorometer (Perkin-Elmer 55B, USA) with a 150-WXenon arc lamp and a Peltier temperature controller (PTP-1 Perkin-Elmer, USA), using a 10 mm quartz cell. DOM synchronous fluorescence spectra (SFS) were measured to identify fluorophores and track changes in DOM fluorescence throughout the experiments. SFS were obtained at 20°C using ASTM1 water (Milli-Q) as blank. Scans were performed over the excitation wavelength range of 250–550 nm (offset value between excitation and emission wavelengths $\Delta\lambda$ = 80 nm; slit width = 10 nm).

2.4 | Laboratory experiments

Two laboratory experiments were performed to study DOM transformation through photo- and biodegradation using DOM leached from soil and leaf litter. Stream water was also used as a DOM source in the photodegradation experiment. All experiments were conducted simultaneously in July 2015, starting immediately after the leachates, and stream water samples were collected. In the photodegradation experiment, incubation of DOM from soil and leaf litter leachates and stream water was performed under two lighting conditions: Dark and PAR+UVR. Five replicates were assigned to each DOM treatment, totalling 30 experimental units. DOM leachates were standardised to a DOC concentration of 4 mg/L by adding Milli-Q water followed by sterilisation by filtration (Millipore PVDF, 0.22 μm pore size, Brazil). Then DOM was poured into pre-combusted quartz tubes (30 ml) and incubated in the environmental test chamber at 20°C with a photoperiod of 14 hr light:10 hr dark. Light was provided by an array of 10 fluorescent tubes (PAR, photosynthetic active radiations), 1 Q-panel

QFS40 (UV-B) and 2 Q-panels 340 (UV-A), placed laterally on three sides of the test chamber, emitting daily doses of 9.17 kJ/m^2 of UV-B, 61.92 kJ/m^2 of UV-A and 75.71 μEm^2/s of PAR. The dark replicates were wrapped with aluminium foil. Experimental units were placed randomly in a vertical wheel and set to rotate at 1 rpm, to ensure their homogenous exposure of the experimental units. After 72 hr of incubation, the samples were filtered (Millipore PVDF, 0.22 μm pore size membranes), and the DOM was characterised.

Biodegradation experiments were performed to study DOM transformation by microbiota. A factorial experiment was conducted with two DOM treatments (soil and leaf litter leachates) and incubated at 10°C, in darkness, for different time periods (t = 0, 2, 4, 6, 8, 12, 18, 24 and 30 days) in a test chamber (Semedic, Argentina). Two DOM treatments were run with three replicates per incubation time (nine), totalling 54 experimental units. Soil and leaf litter leachates (200 ml) with associated microbiota were poured into pre-combusted Erlenmeyer flasks. Nine replicates of Milli-Q water (one per incubation time) were set-up as filter blanks to monitor baseline conditions throughout the experiment. During the experiment, three replicates of each treatment and one control were removed at each established incubation time. A 100 ml sample was taken to measure pH and conductivity, a 50 ml sample was sterilised by filtration and used to measure DOC and DIC concentrations and to perform optical characterisation. The remaining 50 ml of each replicate was preserved with glutaraldehyde (final concentration 1%) to determine bacterial abundance and biomass. These samples were filtered on black membranes (Millipore MSI, 0.22 μm, Brazil) and stained with 4′ 6-diamidino-2-phenylindole (DAPI), following Porter and Feig (1980), for determination of microbial (Bacteria and/or Archaea) abundance and biomass. The filters obtained were mounted on microscope slides using immersion oil for fluorescence microscopy and stored at −20°C. Cells were counted at 1,000× using an epifluorescence microscope (Olympus BX50, USA) equipped with an HBO 50 lamp and a filter for UV excitation. Bacteria size and morphotype characterisation were evaluated from 15 digital images captured in each replicate, using the software Image Pro Plus 4.5 (USA). About 350 cells were measured per filter to determine size, and cell biovolume was calculated following Massana et al. (1997) from two-dimensional size parameters, considering geometric shapes. Biovolume was transformed into carbon biomass using the formula proposed by Norland (1993), derived from Simon and Azam (1989).

2.5 | Data analysis

The absorption coefficients a_{254} and a_{350} were calculated from absorbance scans and normalised by DOC concentration. These coefficients were used as indicators of DOM aromaticity and relative lignin content (a tracer of terrigenous DOM), respectively (Fichot & Benner, 2012; Helms et al., 2014). The spectral slope for the interval 275–295 nm ($S_{275–295}$) was used as an indicator of DOM molecular size and/or as a degradation proxy (Helms et al., 2008; Spencer et al., 2010). The humification index (HIX, Ohno, 2002) was applied to assess the DOM source, diagenesis and sorptive capacity. This index ranges from 0 to 1, with higher values indicating increasing humification. Further information is provided in Supplementary Methods and Table S1.

Excitation–emission matrices (EEMs) were analysed using Parallel Factor Analysis (PARAFAC; Murphy, Stedmon, Wenig, & Bro, 2014), the fluorescence intensities of the main fluorescent peaks being recorded to identify the fluorophores occurring in the different DOM sources. PARAFAC was run with 79 EEMs obtained for the initial characterisation of the leachates and stream water and from all the experiments, using the DOMFluor toolbox for MATLAB®R2014a (Natick, USA). The scatter peaks (Rayleigh and Raman) were removed from the analysis following the methodology proposed by Stedmon and Bro (2008). An exploratory analysis using non-negative constraints was applied to identify and remove outliers from the data set, based on instrument errors, artefacts and discrepancy with other samples, determined by calculating a leverage of 0.5. The number of components discriminated by the PARAFAC was validated by split-half analysis applying 10 random initialisations (Murphy, Stedmon, Graeber, & Bro, 2013). Finally, excitation and emission loadings were used to locate the excitation and emission peaks of the components and their maximum intensity (F_{max}) (Murphy et al., 2013). The relative fluorescence intensity of each component was normalised to the DOC concentration. The excitation and emission spectra obtained through the PARAFAC were checked against the fluorescence spectra in the OpenFluor database (www.openfluor.org, Murphy et al., 2014), to explore their coincidence with components reported in other studies, assuming similarity with a minimum score of 0.95.

One-way ANOVA or t tests were applied to study changes in DOM parameters between radiation treatments in the photodegradation experiment, and between initial and final conditions in the biodegradation experiment. Data were tested for equal variance and normality.

Principal component analysis (PCA) was used to analyse separately the effects of photo- and biodegradation on DOM properties. PCA and correlation tests were performed using the open software Rstudio V3.3.3 (Boston, USA), package FactoMineR. Response variables were log-transformed, centred and standardised for the PCA.

3 | RESULTS

3.1 | Characterisation of DOM from different source materials

Conductivity, pH and DOM concentration and quality differed significantly between source materials (Table 1). Leaf litter leachates showed the lowest mean pH (~5) and highest conductivity (~126 μS/cm^2), followed by soil leachates (~6.4 and 16 μS/cm^2) and stream water (7.4 and 48.4 μS/cm^2). DOC concentration was significantly higher in leaf litter than in soil and stream water samples (Table 1). In the case of the DIC concentration, the opposite pattern

TABLE 1 Physicochemical and dissolved organic matter (DOM) parameters (mean ± 1 *SD*) of natural stream water and soil and leaf litter leachates. Results of the ANOVA comparing parameters between different DOM sources. Letters (a, b, c) indicate different homogeneous groups detected by post hoc comparisons (Holm–Sidak). DOC, dissolved organic carbon concentration; DIC, dissolved inorganic carbon concentration; %Ci, relative contribution of PARAFAC components (C1, C2, C3 and C4) to total fluorescence; A, C, T, M and M_L, DOM fluorescence peaks; EEM, excitation–emission matrix; SFS, synchronous fluorescence spectrum

Features	Stream water (SW)	Soil leachates (SL)	Leaf litter leachates (LL)	One-way ANOVA	Post hoc comparisons SW	SL	LL
DOC (mg/L)	0.7 (0.1)	5.0 (0.6)	304.5 (1.3)	F = 192,533.7*	a	b	c
DIC (mg/L)	4.6 (0.1)	0.8 (0.1)	0.4 (0.1)	F = 2193.8*	a	b	c
DOC:DIC	0.2 (0.1)	6.3 (0.2)	755.0 (33.3)	F = 2228.6*	a	b	c
pH	7.3 (0.1)	6.4 (0.1)	4.9 (0.1)	F = 540.0*	a	b	c
Conductivity ($\mu S/cm^2$)	48.4 (1.5)	15.9 (0.3)	125.8 (1.0)	F = 6973.7*	a	b	c
CDOM features							
a_{254}:DOC (L mg^{-1} m^{-1})	5.81 (0.36)	5.95 (0.11)	3.08 (0.05)	F = 138.9*	a	a	b
a_{350}:DOC (L mg^{-1} m^{-1})	1.58 (0.09)	1.56 (0.03)	0.72 (0.01)	F = 184.5*	a	a	b
$S_{275-295}$ (10^{-3} nm^{-1})	13.57 (0.09)	14.52 (0.04)	17.42 (0.02)	F = 3112.5*	a	b	c
FDOM features							
Humification index	0.95 (0.01)	0.95 (0.01)	0.40 (0.01)	F = 21,569.7*	a	a	b
Total fluorescence (RU)	0.20 (0.01)	1.92 (0.05)	55.20 (0.88)	F = 28.6*	a	b	c
%C1 (A+C)	38.2 (1.2)	41.2 (0.3)	3.6 (0.1)	F = 28.6*	a	b	c
%C2 (T)	6.1 (0.6)	6.4 (0.2)	41.1 (0.1)	F = 7734.6*	a	a	b
%C3 (A+M)	52.8 (0.3)	47.9 (0.5)	10.3 (0.1)	F = 15,566.9*	a	b	c
%C4 (M_L)	3.0 (1.4)	4.5 (0.7)	45.0 (0.2)	F = 1834.9*	a	a	b
C1 (A+C) (RU)	0.08 (0.01)	0.79 (0.03)	1.97 (0.04)	F = 4087.4*	a	b	c
C2 (T) (RU)	0.01 (0.01)	0.12 (0.01)	22.66 (0.41)	F = 28.6*	a	b	c
C3 (A+M) (RU)	0.11 (0.01)	0.92 (0.03)	5.71 (0.10)	F = 28.6*	a	b	c
C4 (M_L) (RU)	0.01 (0.01)	0.09 (0.01)	24.86 (0.43)	F = 28.6*	a	b	c
FDOM plots							
EMM	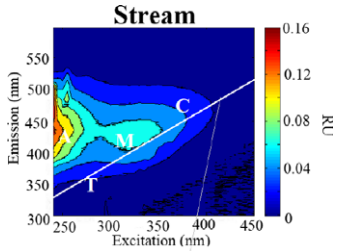	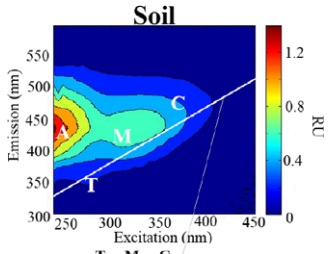	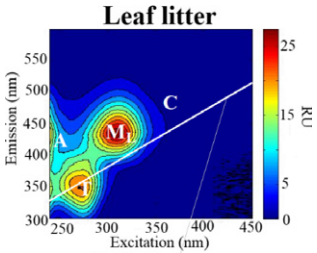				
SFS (RU)	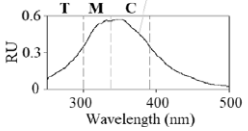	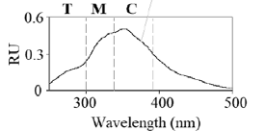	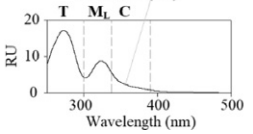				

* = p < .001.

was found, with soil leachates showing the highest values, followed by stream and leaf leachates. Leaf litter DOM showed the highest DOC:DIC ratio, followed by soil and finally stream water (Table 1). The a_{254}:DOC, applied as a proxy for aromaticity, was higher in soil and stream than in leaf litter leachates. A similar trend was found in the a_{350}:DOC, used as an indicator of lignin content and tracer of terrigenous DOC. The $S_{275–295}$ values indicated that the highest DOM molecular size was in stream water, followed by soil and leaf litter samples (Table 1). Humification index was much higher in soil and stream than in leaf litter leachates (Table 1).

The PARAFAC analysis of the EEMs identified four fluorescent components (C1, C2, C3 and C4), which contributed differently to the FDOM of the three sources studied (Table S2). Component 1 showed two excitation maxima at a single emission spectrum, reflecting the combination of fluorescent peaks A and C and matching terrestrially derived material identified previously in different aquatic environments (Tables S1 and S2). C2 was associated with the T-peak and related to a mixture of non-humic compounds comprising proteins, amino acids and phenolic moieties that may be products of the leaching of polyphenols from senescent plants (Kellerman, Kothawala, Dittmar, & Tranvik, 2015; Maie, Scully, Pisani, & Jaffé, 2007). C3, a combination of fluorescent peaks A and M, was probably composed of humic-like compounds derived from biological/microbial activity. C4 was composed of humic substances associated with a particular M peak, differing in its excitation and emission wavelengths from the M peak in C3. This particular M peak prevailed in leaf samples and is mentioned hereafter as M_L. C4 did not match any published component in the OpenFluor database; however, it resembled a component (C5) identified in senescent leaf leachates by Cuss and Guéguen (2015).

Analysis of the relative contribution of the four components to each DOM source showed two distinctive patterns, with the humic components C3 and C1 dominant in stream water and soil leachates, and C2 and C4 prevailing in leaf litter leachates (Table 1).

3.2 | Photodegradation experiment

In general, the DOC concentration of stream water and soil leachates showed negligible change during incubation, regardless of the light treatment. However, leaf litter leachates displayed a slight but significant increase in the DOC under PAR+UVR. The DIC decreased in all DOM sources under PAR+UVR (Table 2). The DOC:DIC ratio increased in the leachates under PAR+UVR, but was stable in stream water. The pH remained stable in all DOM sources and regardless of the light treatment, whereas conductivity was steady in soil DOM, decreased slightly in stream and dropped significantly (~52%) in leaf litter DOM, particularly under PAR+UVR (Table 2).

Exposure to PAR+UVR induced a reduction in molecular size in all DOM sources, reflected by higher $S_{275–295}$ values. In the leachates, a reduction in DOM aromaticity and lignin was inferred through the decrease found in a_{254}:DOC and a_{350}:DOC, respectively. Moreover, significant losses in total fluorescence were detected, and reflected by all four components (Table 2). Under PAR+UVR, C3 decreased more notably in stream and soil leachates, and C4 decreased more in leaf litter leachates, corresponding to degradation of the M and M_L peaks, respectively (Figure 1). C1 was comparatively more photoresistant than the other components, regardless of its source and contribution to total fluorescence (Table 2; Figure 1). C1 (as percentage of total fluorescence; %C1) increased under PAR+UVR, showing greater change in stream water and soil leachates. An increase in %C2 after irradiation was observed only in leaf litter leachates (Table 2).

The two principal components (PC1 and PC2) obtained from the PCA performed to study the effect of photodegradation on different DOM sources accounted for 86.72% of the total variance in the data set (Figure 2). PC1 explained 69.4% of the total variance, being directly correlated with the humic-like components C1 and C3 (C1:DOC, $r = .99$; C3:DOC, $r = .97$), aromaticity (a_{254}:DOC, $r = .98$), lignin content (a_{350}:DOC, $r = .95$) and humification index ($r = .95$), while correlating negatively with molecular weight ($S_{275–295}$, $r = -.75$) and the non-humic components C2 ($r = -.87$) and C4 ($r = -.47$). PC2 accounted for 17.35% of the total variance, with positive correlations with C4 (C4:DOC, $r = .82$) and total fluorescence ($r = .53$), and a negative correlation with molecular weight ($S_{275–295}$, $r = -.60$). PC1 separated the different DOM sources, clustering stream water and soil leachates separately from leaf litter leachates; whereas the effect of irradiation was discriminated along PC1 and PC2. The fresh DOM of leaf litter showed high negative scores with PC1, associated with the higher contribution of C2 and lower molecular weight, grouping at the left side of the plot. In contrast, the humic soil and stream DOM showed a higher contribution of C1 and C3, higher molecular weight, aromaticity, lignin content and humification, clustering at the right (Figure 2). Along PC1, replicates of the PAR+UVR treatment, displaying lower values of aromaticity, lignin content and components C1, C2 and C3, were separated from the dark treatment. PC2 also discriminated the effect of radiation, with PAR+UVR replicates exhibiting lower molecular weight, lower total fluorescence and C4 and grouping separately from unexposed replicates (Figure 2).

3.3 | Biodegradation experiment

The microbial communities growing on soil and leaf litter leachates consisted of three bacterial morphotypes: cocci, short-rod shaped (S-Rod) and long-rod shaped (L-Rod). Total abundance, mean cellular size and total carbon content of these morphotypes were always higher in leaf litter than in soil samples (Tables 3 and S3; Figure S1a, b). Total bacterial abundance increased throughout the experiment in both leachates, with a greater increase in leaf litter (Table 3; Figure S1a,b). In terms of carbon biomass, the microbial assemblage growing in leaf litter DOM was two orders of magnitude higher than in soil DOM after incubation. In soil leachates, the S-Rods were dominant at the beginning of incubation, but later on cocci showed higher biomass, followed by the S-Rods and L-Rods (Figure S1a). In contrast, in leaf litter leachates, the S-Rods and L-Rods codominated the biomass during the first 10 days of incubation, while cocci

TABLE 2 Chemical and DOM parameters (mean ± 1 *SD*) of natural stream water and soil and leaf litter leachates. Results of *t* test comparing irradiation treatments (dark versus PAR+UVR) in the photodegradation experiment. DOC, dissolved organic carbon concentration; DIC, dissolved inorganic carbon concentration; %Ci, relative contribution of PARAFAC components (C1, C2, C3 and C4) to total fluorescence; A, C, T, M and M_L, DOM fluorescence peaks; SFS, synchronous fluorescence spectrum

	Stream			Soil			Leaves		
Features	**Dark**	**PAR+UVR**	***p***	**Dark**	**PAR+UVR**	***p***	**Dark**	**PAR+UVR**	***p***
DOC (mg/L)	0.73 (0.05)	0.66 (0.06)	ns	4.04 (0.05)	4.03 (0.03)	ns	4.2 (0.1)	4.3 (0.1)	*
DIC (mg/L)	4.61 (0.12)	4.51 (0.01)	ns	0.65 (0.06)	0.59 (0.06)	ns	0.38 (0.01)	0.35 (0.01)	*
DOC:DIC	0.2 (0.1)	0.2 (0.1)	ns	6.3 (0.6)	6.9 (0.6)	ns	11.1 (0.5)	12.5 (0.4)	**
pH	7.3 (0.1)	7.4 (0.1)	ns	6.2 (0.1)	6.3 (0.1)	ns	5.6 (0.1)	5.6 (0.2)	ns
Conductivity ($\mu S/cm^2$)	48.4 (1.5)	46.5 (0.7)	*	16.7 (5.6)	17.1 (3.2)	ns	16.7 (3.4)	8.0 (0.7)	**
CDOM features									
a_{254}:DOC (L mg^{-1} m^{-1})	5.81 (0.36)	5.93 (0.35)	ns	6.60 (0.10)	5.35 (0.07)	**	3.79 (0.05)	3.31 (0.03)	**
a_{350}:DOC (L mg^{-1} m^{-1})	1.58 (0.09)	1.49 (0.12)	ns	1.82 (0.03)	1.34 (0.01)	*	1.02 (0.02)	0.92 (0.05)	*
$S_{275–295}$ (10^{-3} nm^{-1})	13.57 (0.09)	17.65 (0.23)	**	13.91 (0.08)	17.72 (0.05)	**	18.11 (0.11)	21.32 (0.41)	*
FDOM features									
Humification index	0.95 (0.01)	0.95 (0.01)	ns	0.97 (0.01)	0.97 (0.01)	ns	0.32 (0.01)	0.44 (0.03)	**
Total fluorescence (RU)	0.20 (0.01)	0.15 (0.01)	**	1.65 (0.03)	1.10 (0.01)	**	1.08 (0.09)	0.44 (0.01)	*
%C1 (A+C)	38.2 (1.2)	44.7 (0.5)	**	42.1 (0.4)	51.5 (0.3)	**	9.2 (0.9)	16.7 (1.1)	*
%C2 (T)	6.1 (0.6)	4.9 (0.2)	*	3.3 (0.7)	2.0 (0.3)	*	49.7 (1.5)	56.5 (1.5)	*
%C3 (A+M)	52.8 (0.3)	50.4 (0.5)	**	49.6 (0.7)	46.6 (0.4)	**	5.8 (1.2)	2.9 (0.8)	*
%C4 (M_L)	3.0 (1.4)	0.0 (0.0)	*	5.0 (0.8)	0.0 (0.0)	*	35.2 (1.8)	23.9 (0.5)	**
C1 (A+C) (RU)	0.08 (0.01)	0.06 (0.01)	**	0.69 (0.01)	0.57 (0.01)	**	0.10 (0.01)	0.07 (0.01)	**
C2 (T) (RU)	0.01 (0.01)	0.01 (0.01)	**	0.05 (0.01)	0.02 (0.01)	**	0.54 (0.06)	0.25 (0.01)	*
C3 (A+M) (RU)	0.11 (0.01)	0.07 (0.01)	**	0.82 (0.02)	0.51 (0.01)	**	0.06 (0.02)	0.01 (0.01)	*
C4 (M_L) (RU)	0.01 (0.01)	0.00 (0.00)	*	0.08 (0.01)	0.00 (0.00)	*	0.38 (0.01)	0.11 (0.01)	**
FDOM plots									
SFS (RU)	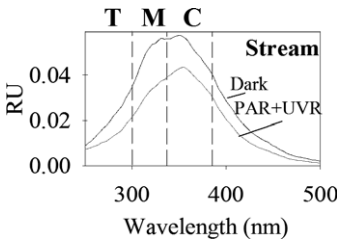			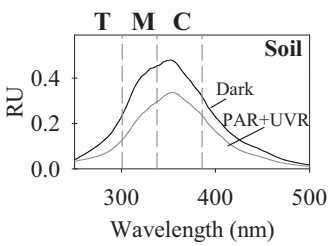			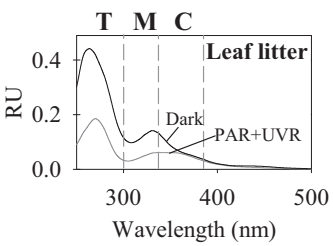		

* = $p < .05$; ** = $p < .001$; ns = $p > .05$.

showed the highest biomass later on (Figure S1b). At the end of incubation, the biomass in soil and leaf litter leachates was dominated by cocci (~50 and 63%, respectively), followed by S-Rods (~29% and 30%) and L-Rods (~19% and 8%) (Table 3; Figure S1a,b).

During the experimental exposure, DOC concentration was significantly reduced by microbial activity, especially in leaf litter DOM (~53%). DIC concentration remained stable during the first week of incubation in leaf litter leachates, subsequently increasing up to ~975%. In soil samples, the DOC and DIC concentrations decreased during incubation, although the change was less pronounced than in leaf leachates (~24% and ~13%, respectively) (Table 3; Figure S1c,d). Conductivity decreased sharply in leaf litter leachates and moderately in soil, while pH presented the opposite pattern (Table 3).

During leachate incubation, CDOM and FDOM exhibited clear signs of biodegradation, reflected by increasing aromaticity, lignin content (a_{254}:DOC and a_{350}:DOC, respectively) and molecular weight (lower $S_{275–295}$), although changes were more pronounced in leaf litter leachates (Table 3; Figure S1e,f). During leaf litter DOM incubation, the intensity of components C4, C2 and C3 decreased substantially, while C1 increased (Figures 3 and S1h). This pattern clearly reflects humification, which was also indicated by decreasing values of the M_L and T peaks, along with an increase in the C peak (Table 3). Furthermore, at the end of the experiment, the contribution of humic component C1 was threefold higher than at the beginning of incubation. In soil DOM, the intensity of all the components decreased, but the change was greater in C2 (T peak) (Figure S1g). At the end of the biodegradation experiment, a reduction of the T

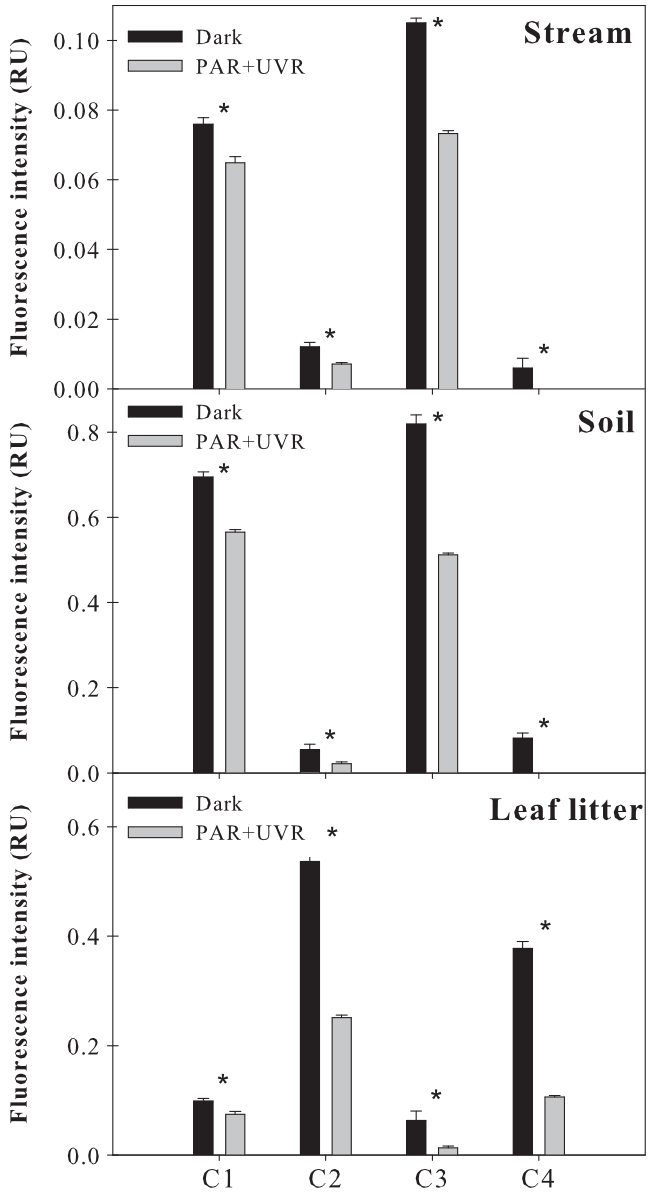

FIGURE 1 Changes in the fluorescence intensity of the PARAFAC components (C1, C2, C3 and C4) present in stream water and soil and leaf litter leachates in the different irradiation treatments of the photodegradation experiment. Bars are mean values (±1 *SD*; n = 4–5). * = $p < .05$ (*t* test)

peak was observed in the synchronous fluorescence spectra (Table 3).

The first and second principal components (PC1 and PC2) of the PCA performed to analyse the biodegradation process accounted to explain 93.5% of the data set variation (Figure 4). PC1 explained 80.3% and the variables correlating positively were total fluorescence (r = .99), DOC concentration (r = .99), C4:DOC (r = .97), C2:DOC (r = .96) and the $S_{275–295}$ (r = .94). The variables correlating negatively with this axis were humification (r = −.99), a_{254}:DOC (r = −.99), a_{350}:DOC (r = −.81), C3:DOC (r = .99) and C1:DOC (r = .98). PC2 explained 13.2% of the total variance, correlating positively with DIC concentration (r = .94), bacterial biomass (r = .54) and a_{350}:DOC (r = .54). PC1 discriminated DOM sources, with the fresher DOM of leaf litter clustering on the right side of the plot and soil leachates grouping on the left (Figure 4). In leaf samples, the effect of biodegradation was apparent along both axes, showing progressive humification, reflected by increasing DIC, C1, a_{254}:DOC, a_{350}:DOC, molecular weight ($S_{275–295}$) and bacterial biomass, and decreasing DOC, C2 and C4. Although the change in optical parameters overall was lower in soil DOM, it showed the same trend.

Bacterial biomass was negatively correlated with DOC and total fluorescence in both leachates, indicating the transfer of carbon from the DOM pool to the microbiota. In leaf litter DOM, the negative correlation between bacterial biomass C2 (T peak) and C4 (M_L peak) reflected their biolability, while the negative correlation with C1 and the positive correlation with aromaticity and lignin content indicated humification (Figure S2). In soil DOM, the negative correlation between bacterial biomass and C2, and the lack of correlation with the other components, suggested the refractory condition and limited biolability of this source, which was also supported by positive correlations with bacterial biomass and molecular weight (Figure S2).

4 | DISCUSSION

Leaf litter and soil leachates showed different contributions of DOM in terms of concentration and quality. Leaf and soil samples yielded contrasting amounts of DOC, ~300 mg/L and ~5 mg/L, respectively. In contrast, DIC concentration in soil leachates was twofold higher (0.8 mg/L) than in leaf litter (0.4 mg/L). In stream water, DOC was much lower (0.7 mg/L) while DIC was the highest recorded (4.6 mg/L) (Table 1). The distinctive DOC:DIC of the leachates and stream water reflects a processing gradient, with the fresher DOM of leaf litter showing the lowest level of processing (highest DOC:DIC ratio), increasing towards soil and finally to stream water (Table 1). This DOM processing gradient was also detected through optical parameters. The leachates and stream water displayed overall high molecular weight ($S_{275–295} > 13{\cdot}10^{-3}$ nm^{-1}), characteristic of terrestrially derived DOM (Helms et al., 2008; Spencer et al., 2010), although differences between sources were apparent. Soil and stream DOM showed greater humification, reflected by their high aromaticity and lignin content and higher humification index, contrasting with the fresher DOM from leaf litter (Tables 1 and S1). The different DOM amounts and quality yielded by soil and leaf indicated the increasing natural loss of hydrosoluble compounds from the end-member (leaves) to the soil. Moreover, the similarity observed between stream and soil leachates revealed the importance of soil DOM to stream water. The lower DOC and higher DIC of stream water in relation to the leachates suggested a continuum in DOM loss/transformation from the terrestrial towards the aquatic compartment. In fact, DOM from leaf biomass has been shown to contain labile and low molecular weight organic substances (e.g., amino acids, soluble phenols), carbohydrates, and phenolic compounds derived from tannins and lignin (Chen & Jaffé, 2016; Cuss & Guéguen, 2015; Maie et al., 2007), which are preferentially transformed at the soil surface (Uselman, Qualls, & Lilienfein, 2012). The leaching of water-soluble

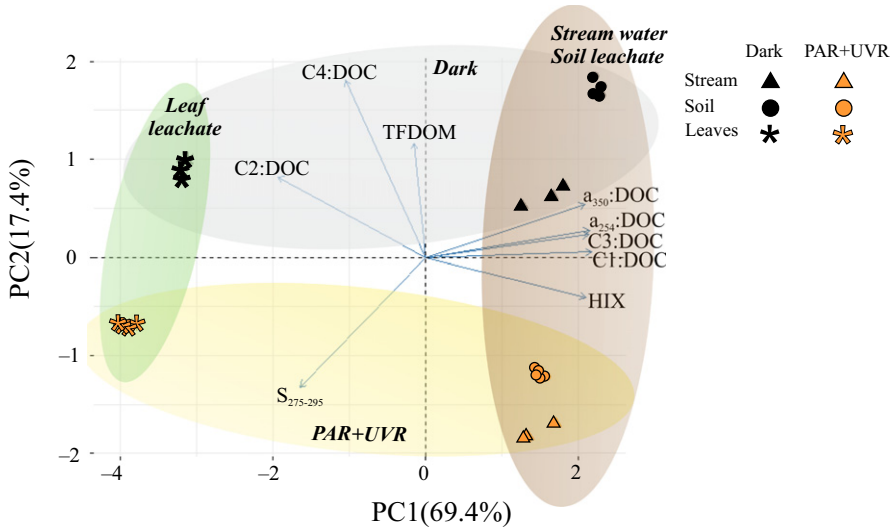

FIGURE 2 Plot of the two principal components (PC1 and PC2) obtained in the principal component analysis (PCA) including CDOM and FDOM parameters (a_{254}:DOC, a_{350}:DOC, $S_{275–295}$, HIX and DOC-normalised PARAFAC components) in the photodegradation experiment. HIX, humification index; TFDOM: Total fluorescence of dissolved organic matter

compounds to deeper soil strata and microbial use/generation of labile/humic DOM produce the accumulation of recalcitrant compounds in the upper soil horizon (Hur, Park, & Schlautman, 2009; Kalbitz et al., 2003; Michel et al., 2006). Thus, topsoil DOM retains comparatively more hydrophobic compounds, including a higher proportion of less labile aromatic molecules with a history of processing (Kaiser & Kalbitz, 2012; Kalbitz et al., 2003).

The fluorescent components dominating the DOM pool of soil and stream were the humic C1 (A+C peaks) and C3 (A+M peaks), whereas the humic C4 (M_L peak) and the non-humic compound C2 (T peak) prevailed in leaf litter DOM. C3 and C4 are both comprised in the M peak region (M peak in soil leachates and stream and M_L peak in leaf samples). The slight shift in the Em/Ex coordinates of these peaks is probably due to their different degree of processing (Tables 1, S1 and S2). In the case of the leachates, C2 (T peak) can certainly be attributed to compounds from the degradation of vascular plant leachates, such as tannins and lignins. Non-protein compounds, such as propylphenol monomers (that build up lignin present in vascular plant leachates) and tannins, fluoresce in the low-UV region of the EEM (Hansen et al., 2016; Hernes, Bergamaschi, Eckard, & Spencer, 2009; Maie et al., 2007).

The humic components C1 and C3 and non-humic C2 have been found in DOM from aquatic systems of the same catchment (Table S2). The DOM of these Andean systems is predominantly allochthonous, and the temporal variation of its components is related to changing terrestrial inputs and photochemical and biological degradation (Garcia, Reissig, et al., 2015; Garcia, Diéguez, & Queimaliños, 2015; Soto Cárdenas et al., 2017). The C4 recorded in DOM leached from *N. pumilio* leaves does not match any component included in OpenFluor because this database comprises so far exclusively aquatic DOM components. Nevertheless, C4 matches one component described by Cuss and Guéguen (2015) in leachates of senescent maple leaves. We consider that C4 degradation contributes to the humic C1 and C3 prevailing in soil leachates and stream water.

Our experiments focused on photochemical and biological transformation patterns of DOM from different sources. Photodegradation of leachates and stream water showed little to negligible change in DOC (Table 2). The different DOM sources exhibited decay in absorbance and fluorescence, which was more pronounced in leaf litter leachates than in soil and stream, probably due to the photoreduction of chromophores (Chen & Jaffé, 2016; Helms et al., 2008, 2014). A general decrease in molecular weight, aromaticity and lignin content was detected in the leachates (Table 2; Figure 2). The increase in DOM spectral slopes following irradiation has been attributed to a shift from high molecular weight to low molecular weight compounds in natural waters (Helms et al., 2008, 2014; Spencer et al., 2009) and also in soil and biomass extracts (Chen & Jaffé, 2016; Fellman et al., 2013; Hansen et al., 2016). The molecular weight and aromaticity of compounds are related to molar absorptivity, and photodegradation decreases both parameters in terrigenous CDOM (Aiken, 2014; Fichot & Benner, 2012; Helms et al., 2008, 2014). Lignin in particular is a highly photoreactive biopolymer (Fichot & Benner, 2012; Fichot et al., 2016; Ishii & Boyer, 2012) that can be completely degraded under natural radiation (Spencer et al., 2009).

In our photodegradation experiment, we observed a change towards higher humification, particularly in leaf litter DOM. In contrast, soil and stream DOM remained almost unchanged, indicating the higher photoresistance of their prevailing components C1 and C3 (Table 2; Figure 2). In leaf litter samples, C2 and C4 (M_L peak) decreased, but the latter was more readily photodegraded. The smaller decrease in C2 may represent a trade-off between its photodegradation and photoproduction from C4. Photoreduction of humic substances such as C4 generates compounds of low molecular weight, such as the non-humic T-peak (Maie et al., 2007; Stubbins et al., 2010). In soil and stream DOM, C3 decreased more than C1; thus, the higher photoresistance of soil leachates and stream water may be related to prevalence of the humic C1 (Figure 1).

In the experimental conditions applied, DOM from stream water displayed recalcitrance. However, we cannot rule out the possibility that longer exposure to radiation could promote further degradation. Other studies have reported almost complete degradation of

TABLE 3 Physicochemical and DOM parameters and microbial community features (mean ± 1 *SD*) of soil and leaf litter leachates exposed to biodegradation. Results of the statistical analysis (*t* test) comparing initial (day 0) versus final (day 30) conditions in the biodegradation experiment. DOC, dissolved organic carbon concentration; DIC, dissolved inorganic carbon concentration; %Ci, relative contribution of PARAFAC components (C1, C2, C3 and C4) to total fluorescence; SFS, synchronous fluorescence spectrum

	Soil leachates			Leaf litter leachates		
Features	**Initial**	**Final**	***p***	**Initial**	**Final**	***p***
DOC (mg/L)	5.01 (0.06)	3.84 (0.16)	**	304.5 (1.3)	145.3 (4.4)	**
DIC (mg/L)	0.79 (0.02)	0.69 (0.08)	*	0.40 (0.02)	3.95 (0.16)	*
DOC:DIC	6.3 (0.2)	5.6 (0.4)	*	755.0 (33.3)	36.8 (1.4)	**
pH	6.4 (0.1)	6.6 (0.2)	ns	4.9 (0.1)	7.4 (0.1)	**
Conductivity ($\mu S/cm^2$)	15.9 (0.3)	15.0 (1.5)	ns	125.8 (1.0)	96.0 (3.2)	**
CDOM features						
a_{254}:DOC (L mg^{-1} m^{-1})	5.95 (0.11)	6.90 (0.17)	*	3.08 (0.05)	5.16 (0.08)	**
a_{350}:DOC (L mg^{-1} m^{-1})	1.56 (0.03)	1.87 (0.05)	*	0.72 (0.01)	1.75 (0.03)	**
$S_{275–295}$ (10^{-3} nm^{-1})	14.52 (0.04)	13.80 (0.04)	**	17.42 (0.02)	14.98 (0.04)	**
FDOM features						
Humification index	0.95 (0.01)	0.97 (0.01)	**	0.40 (0.01)	0.54 (0.01)	**
Total fluorescence (RU)	1.92 (0.05)	1.69 (0.10)	*	55.20 (0.88)	21.90 (0.80)	**
%C1 (A+C)	41.2 (0.3)	43.1 (0.3)	**	3.6 (0.1)	17.0 (0.9)	**
%C2 (T)	6.4 (0.2)	2.8 (0.3)	**	41.1 (0.1)	41.5 (0.4)	ns
%C3 (A+M)	47.9 (0.5)	49.5 (0.5)	*	10.3 (0.1)	14.3 (0.3)	**
%C4 (M_L)	4.5 (0.7)	4.5 (0.8)	ns	45.0 (0.2)	27.1 (0.6)	**
C1 (A+C) (RU)	0.79 (0.03)	0.73 (0.05)	ns	1.97 (0.04)	3.73 (0.25)	**
C2 (T) (RU)	0.12 (0.01)	0.05 (0.01)	**	22.66 (0.41)	9.09 (0.26)	**
C3 (A+M) (RU)	0.92 (0.03)	0.84 (0.05)	ns	5.71 (0.10)	3.14 (0.17)	**
C4 (M_L) (RU)	0.09 (0.01)	0.08 (0.01)	ns	24.86 (0.43)	5.94 (0.25)	**
Microbial community parameters						
Total abundance (10^6 cell/ml)	1.51 (0.14)	3.67 (1.09)	*	0.04 (0.01)	66.00 (10.23)	**
%Cocci abundance	61.6 (3.8)	71.9 (0.5)	*	80.0 (1.5)	70.4 (4.0)	*
%S-rod abundance	31.4 (3.0)	20.4 (0.7)	*	12.6 (1.9)	24.5 (3.6)	*
%L-rod abundance	7.0 (1.4)	7.7 (0.6)	ns	7.4 (0.6)	5.1 (0.8)	*
Total biomass (10^4 pg Carbon/ml)	2.69 (0.17)	5.40 (1.25)	*	0.12 (0.03)	178.80 (26.57)	**
%Cocci biomass	40.1 (3.8)	51.1 (0.7)	*	38.5 (1.4)	62.7 (4.5)	**
%S-rod biomass	45.5 (3.1)	29.4 (1.1)	**	23.3 (3.3)	29.5 (3.9)	ns
%L-rod biomass	14.4 (2.6)	19.4 (1.4)	*	38.2 (2.9)	7.8 (1.2)	**
FDOM plots						
SFS (RU)	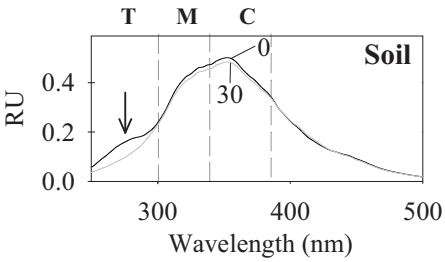			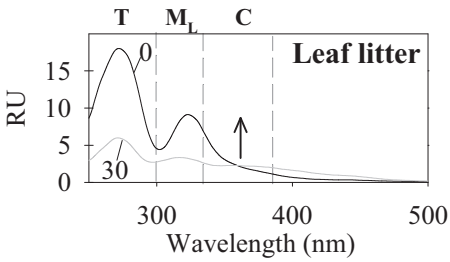		

* = $p < .05$; ** = $p < .001$; ns: $p > .05$.

recalcitrant allochthonous DOM under long-term exposure to radiation (Fichot et al., 2016; Helms et al., 2014).

The biodegradation experiment showed high consumption of DOC by bacteria. Soil DOM was comparatively more biorecalcitrant than leaf litter DOM (Figure 4), as indicated by the higher growth (abundance and biomass) of bacteria in leaf litter leachates and higher DOC consumption and DIC production (Table 3; Figures 4 and S1). Moreover, bacterial morphotypes growing in leaf samples were

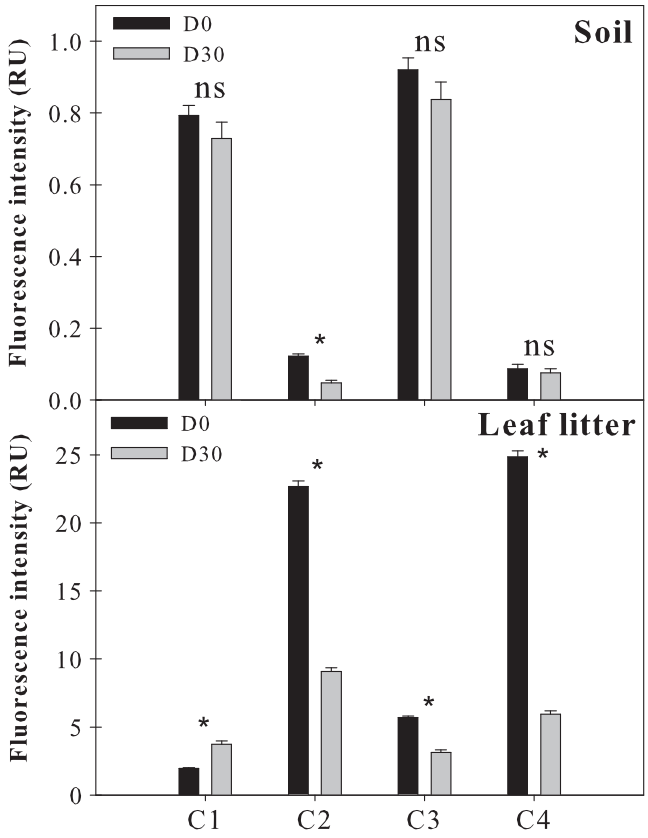

FIGURE 3 Changes in the fluorescence intensity of the PARAFAC components (C1, C2, C3 and C4) present in soil and leaf leachates at initial and final times in the biodegradation experiment. C1 = peaks A+C; C2 = peak T; C3 = peaks A+M; C4 = M_L. Bars are mean values (±1 *SD*; $n = 3$). * = $p < .05$; ns = $p > .05$ (*t* test)

comparatively larger and had higher carbon content (Table S3). The L- and S-rods were more abundant in leaf litter leachates, while S-rods prevailed in soil samples as long as labile DOM was available. Cocci outnumbered other morphotypes when humic biorecalcitrant material had built-up (Figure S1). Differences in bioreactivity in the DOM sources were reflected in the DOC:DIC ratio, which decreased ~95% in leaf litter and ~12% in soil. The increasing DIC values indicated progressive DOC mineralisation due to microbial processing.

Changes in DOM quality due to microbial activity showed similar trends regardless of DOM source, although it was greater in leaf DOM (Table 3; Figures 4 and S1). Biodegradation caused humification, reflected by increasing molecular weight and lignin content throughout incubation. This was probably because of the selective consumption of accessible compounds and the production of biorefractory humic substances, showing the dual role of microorganisms as consumers and producers, as has been pointed out in the literature (Fasching, Behounek, Singer, & Battin, 2014; Guillemette & del Giorgio, 2012).

In the biodegradation experiment, the total fluorescence decreased sharply. However, a greater change occurred in leaf DOM, due to the fact that C2, and to an even greater extent C4, was consumed by bacteria. The smaller decrease in C2 may be due to a trade-off between its consumption and generation, since bacteria can be a source of and/or a sink for amino acid-like and humic-like DOM (Cory & Kaplan, 2012). In leaf litter leachates, C1 increased by the end of incubation (Table 3; Figure S1), perhaps due to accumulation of a subproduct of C4. The higher biodegradability of leaf DOM is probably based on its content of biolabile components (C2 and C4), whereas the higher biorecalcitrance of soil DOM is due to the prevalence of refractory components (C1 and C3). The reactivity gradient observed goes from the biolabile C2 and C4 towards the less reactive and more biorecalcitrant C1 and C3 (Figures 3 and S1). During biodegradation, labile components are consumed first, leaving behind more recalcitrant/unreactive compounds and generating less labile subproducts (Guillemette & del Giorgio, 2012; Kellerman et al., 2015; Yamashita & Tanoue, 2008). DOM leached from leaves is composed of small biodegradable molecules and larger non-humic compounds such as carbohydrates and proteins, while soil DOM is rich in refractory humic substances and macromolecules (Chen & Jaffé, 2016; Hur et al., 2009; Maie et al., 2007).

Overall, the photo- and biodegradation of terrestrial material produced humification, as observed in other studies (e.g., Chen & Jaffé, 2016; and references therein). Leaf litter, soil and stream DOM showed an increasing gradient of humification and decreasing reactivity. Thus, leaf litter and stream water DOM can be considered end-members, whereas soil DOM appears to be intermediate in this reactivity continuum. Leaf litter signatures were not found in stream water and thus may not be appropriate for tracking terrestrial inputs. DOM leached from plants is degraded first in the soil, and DOM from soils probably makes the largest contribution to stream DOM,

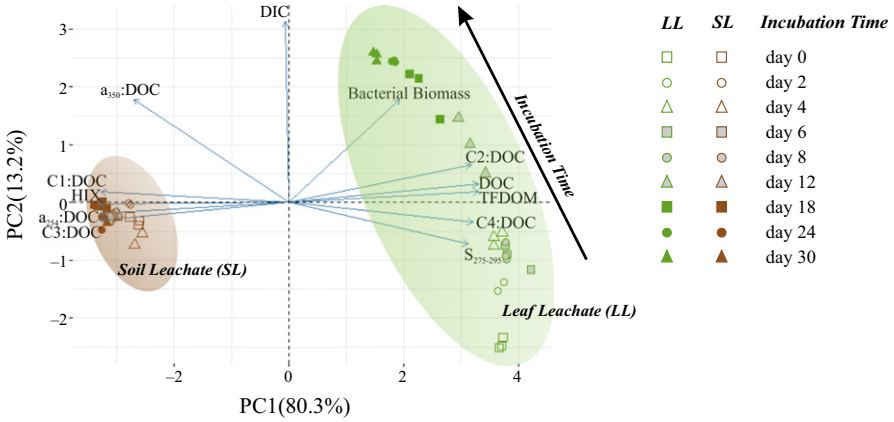

FIGURE 4 Plot of the two principal components obtained in the principal component analysis (PCA) including CDOM and FDOM parameters (a_{254}:DOC, a_{350}:DOC, $S_{275–295}$, HIX and DOC-normalised PARAFAC components and bacteria biomass) in the biodegradation experiment. HIX, humification index; TFDOM: Total fluorescence of dissolved organic matter

as reflected by their similar signatures and close position in the reactivity continuum. Terrestrial inputs to aquatic systems are known to be transformed by microbial processes in the soil up to the point of not being recognisable as deriving from terrestrially fixed carbon (Marín-Spiotta et al., 2014). Nevertheless, the DOC:DIC ratio clearly indicates lower carbon mineralisation in soil leachates (6.3) than in stream water (0.2). In the natural environment, the contrasting DOC and DIC concentrations in soil leachates and streams may promote a reactivity shift, particularly in the soil–stream interphase (Hutchins et al., 2017).

Headwaters of Andean Patagonia show extremely low DOC and nutrient levels and clear signs of allochthony (Garcia, Diéguez, et al., 2015; Garcia, Reissig, et al., 2015; Queimaliños et al., 2012; Soto Cárdenas et al., 2017). Our results showed that DOM leaching from leaf litter of *N. pumilio* provides labile carbon that is processed in the soils and delivered to the headwater network. Signs of fresh DOM from leaf litter are not apparent during base-flow conditions in low order streams. In fact, stream DOM is highly humic and similar in composition with soil DOM. However, spring snowmelt delivers terrestrial DOM enriched with the non-humic T peak derived from less processed leaves dropped in autumn. These leaves remain under snow cover for several months, which slows down leaching and degradation on topsoils (Garcia, Reissig, et al., 2015).

Andean Patagonian aquatic food webs sustain microbial communities adapted to extremely low nutrient and DOC levels, and which rely on allochthonous DOM inputs (Gerea et al., 2016). Natural photochemical processing enhanced by high solar radiation levels generates labile compounds from allochthonous DOM (Soto Cárdenas et al., 2017; Zagarese et al., 2001). This mechanism operates in Andean lakes where cumulative photodegradation breaks down humic allochthonous DOM into non-humic low molecular weight compounds, particularly in the dry season (Queimaliños et al., 2012; Soto Cárdenas et al., 2017). Overall, photo- and biodegradation gradually transform terrestrial DOM, which becomes more similar to aquatic DOM. This pattern has been found in several studies focusing on the effects of photo- and biodegradation in different DOM sources (Chen & Jaffé, 2014; Hansen et al., 2016; Hur et al., 2009).

Analysis of the processes transforming DOM contributes to our understanding of the pathways of carbon fluxes between Earth's compartments (Battin et al., 2009). Our study recognised a potential DOM pathway in a pristine Andean Patagonian catchment, from terrestrial biomass to soils and aquatic systems, highlighting a DOM reactivity continuum in which photo- and biodegradation both intervene. Furthermore, our results highlight the importance of the carbon pulses from *N. pumilio* litter falling into the soils and headwaters in Andean catchments, and the impact of degradation on the fate of this terrestrial carbon supply. As far as we know, this is the first study to characterise the quality of DOM supplied by leaf litter and soil from native *N. pumilio* deciduous forest to headwaters of Andean Patagonia, identifying photo- and biodegradation prints and a potential environmental continuum in DOM reactivity. Further experimentation combining photo- and biodegradation (alternately and/or sequentially) could provide better understanding of DOM transformation from terrestrial sources to aquatic systems and identify characteristics of the reactivity continuum more precisely.

Sustained warming and drying in Andean Patagonia (Villalba et al., 2012) are likely to have an effect on *N. pumilio* treelines through regulation of seedling establishment and growth (Daniels & Veblen, 2004). Moreover, forecasted climatic changes in this region, particularly the reduction in precipitation to the east of the Andes, would affect the hydrology (Masiokas et al., 2008) and connectivity between terrestrial and aquatic systems, impacting the carbon flux within headwater catchments.

ACKNOWLEDGMENTS

This study was funded by PIP 2011-0064 (M.C. Diéguez), PICT 2013-1384 (M. Reissig), PICT 2015-0066 (P.E. García), PICT 2015-3496 (C.P. Queimaliños) and PICT 2016-0499 (M.C. Diéguez). The Administration of Nahuel Huapi National Park and San Carlos de Bariloche Town Council granted permission to collect samples. We are grateful to G.L. Pérez and C.P. Queimaliños for fruitful discussions and to C. Connon and A. Shaw for the revision of the English language. The authors are CONICET researchers.

ORCID

Roberto Daniel Garcia http://orcid.org/0000-0001-7216-4723

REFERENCES

Aiken, G. R. (2014). Fluorescence and dissolved organic matter: A chemist's perspective. In P. Coble, J. Lead, A. Baker, D. Reynolds, & R. Spencer (Eds.), *Aquatic organic matter fluorescence* (pp. 35–74). New York, NY: Cambridge University Press. https://doi.org/10.1017/CBO9781139045452

Albariño, R. J., Díaz Villanueva, V., & Buria, L. (2009). Leaf litter dynamics in a forested small Andean catchment, Northern Patagonia, Argentina. In C. Oyarzún, N. Verhoest, P. Boeckx, & R. Godoy (Eds.), *Ecological advances on Chilean temperate rainforests* (pp. 183–211). Gent, Belgium: Academia Press.

Aufdenkampe, A. K., Mayorga, E., Raymond, P. A., Melack, J. M., Doney, S. C., Alin, S. R., … Yoo, K. (2011). Riverine coupling of biogeochemical cycles between land, oceans, and atmosphere. *Frontiers in Ecology and the Environment*, *9*, 53–60. https://doi.org/10.1890/100014

Battin, T. J., Luyssaert, S., Kaplan, L. A., Aufdenkampe, A. K., Richter, A., & Tranvik, L. J. (2009). The boundless carbon cycle. *Nature Geoscience*, *2*, 598–600. https://doi.org/10.1038/ngeo618

Benner, R., & Kaiser, K. (2011). Biological and photochemical transformations of amino acids and lignin phenols in riverine dissolved organic matter. *Biogeochemistry*, *102*, 209–222. https://doi.org/10.1007/s10533-010-9435-4

Chen, M., & Jaffé, R. (2014). Photo- and bio-reactivity patterns of dissolved organic matter from biomass and soil leachates and surface waters in a subtropical wetland. *Water Research*, *61*, 181–190. https://doi.org/10.1016/j.watres.2014.03.075

Chen, M., & Jaffé, R. (2016). Quantitative assessment of photo-and bioreactivity of chromophoric and fluorescent dissolved organic matter from biomass and soil leachates and from surface waters in a subtropical wetland. *Biogeochemistry*, *129*, 273–289. https://doi.org/10.1007/s10533-016-0231-7

Cole, J. J., Prairie, Y. T., Caraco, N. F., McDowell, W. H., Tranvik, L. J., Striegl, R. G., … Melack, J. (2007). Plumbing the global carbon cycle: Integrating inland waters into the terrestrial carbon budget. *Ecosystems*, *10*, 172–185. https://doi.org/10.1007/s10021-006-9013-8

Cory, R. M., & Kaplan, L. A. (2012). Biological lability of streamwater fluorescent dissolved organic matter. *Limnology and Oceanography*, *57*, 1347–1360. https://doi.org/10.4319/lo.2012.57.5.1347

Cuss, C. W., & Guéguen, C. (2013). Distinguishing dissolved organic matter at its origin: Size and optical properties of leaf-litter leachates. *Chemosphere*, *92*, 1483–1489. https://doi.org/10.1016/j.chemosphere.2013.03.062

Cuss, C. W., & Guéguen, C. (2015). Characterizing the labile fraction of dissolved organic matter in leaf leachates: Methods, indicators, structure, and complexity. In Z. He, & F. Wu (Eds.), *Labile organic matter—Chemical compositions, function, and significance in soil and the environment* (pp. 237–274). Madison, WI: SSSA Spec. Publ. Press.

Daniels, L. D., & Veblen, T. T. (2004). Spatiotemporal influences of climate on altitudinal treeline in northern Patagonia. *Ecology*, *85*, 1284–1296. https://doi.org/10.1890/03-0092

Fasching, C., Behounek, B., Singer, G. A., & Battin, T. J. (2014). Microbial degradation of terrigenous dissolved organic matter and potential consequences for carbon cycling in brown-water streams. *Scientific Reports*, *4*, 1–7.

Fasching, C., Ulseth, A. J., Schelker, J., Steniczka, G., & Battin, T. J. (2016). Hydrology controls dissolved organic matter export and composition in an Alpine stream and its hyporheic zone. *Limnology and Oceanography*, *61*, 558–571. https://doi.org/10.1002/lno.10232

Fellman, J. B., Petrone, K. C., & Grierson, P. F. (2013). Leaf litter age, chemical quality, and photodegradation control the fate of leachate dissolved organic matter in a dryland river. *Journal of Arid Environments*, *89*, 30–37. https://doi.org/10.1016/j.jaridenv.2012.10.011

Fichot, C. G., & Benner, R. (2012). The spectral slope coefficient of chromophoric dissolved organic matter ($S_{275–295}$) as a tracer of terrigenous dissolved organic carbon in river-influenced ocean margins. *Limnology and Oceanography*, *57*, 1453. https://doi.org/10.4319/lo.2012.57.5.1453

Fichot, C. G., Benner, R., Kaiser, K., Shen, Y., Amon, R. M., Ogawa, H., … Lu, C. (2016). Predicting dissolved lignin phenol concentrations in the coastal ocean from chromophoric dissolved organic matter (CDOM) absorption coefficients. *Frontiers in Marine Science*, *3*, 1–15.

Garcia, P. E., Diéguez, M. C., & Queimaliños, C. (2015). Landscape integration of North Patagonian mountain lakes: A first approach using characterization of dissolved organic matter. *Lakes & Reservoirs: Research & Management*, *20*, 19–32. https://doi.org/10.1111/lre.12083

Garcia, R. D., Reissig, M., Queimaliños, C. P., Garcia, P. E., & Diéguez, M. C. (2015). Climate-driven terrestrial inputs in ultraoligotrophic mountain streams of Andean Patagonia revealed through chromophoric and fluorescent dissolved organic matter. *Science of the Total Environment*, *521*, 280–292. https://doi.org/10.1016/j.scitotenv.2015.03.102

Garreaud, R., Lopez, P., Minvielle, M., & Rojas, M. (2013). Large-scale control on the Patagonian climate. *Journal of Climate*, *26*, 215–230. https://doi.org/10.1175/JCLI-D-12-00001.1

Gerea, M., Pérez, G., Unrein, F., Soto Cárdenas, C., Morris, D., & Queimaliños, C. P. (2016). CDOM and the underwater light climate in two shallow North Patagonian lakes: Evaluating the effects on nano and microphytoplankton community structure. *Aquatic Sciences*, *79*, 231–248.

Guillemette, F., & del Giorgio, P. A. (2012). Simultaneous consumption and production of fluorescent dissolved organic matter by lake bacterioplankton. *Environmental Microbiology*, *14*, 1432–1443. https://doi.org/10.1111/j.1462-2920.2012.02728.x

Haei, M., Rousk, J., Ilstedt, U., Öquist, M., Bååth, E., & Laudon, H. (2011). Effects of soil frost on growth, composition and respiration of the soil microbial decomposer community. *Soil Biology and Biochemistry*, *43*, 2069–2077. https://doi.org/10.1016/j.soilbio.2011.06.005

Hansen, A. M., Kraus, T. E., Pellerin, B. A., Fleck, J. A., Downing, B. D., & Bergamaschi, B. A. (2016). Optical properties of dissolved organic matter (DOM): Effects of biological and photolytic degradation. *Limnology and Oceanography*, *61*, 1015–1032. https://doi.org/10.1002/lno.10270

Helms, J. R., Mao, J., Stubbins, A., Schmidt-Rohr, K., Spencer, R. G., Hernes, P. J., … Mopper, K. (2014). Loss of optical and molecular indicators of terrigenous dissolved organic matter during long-term photobleaching. *Aquatic Sciences*, *76*, 353–373. https://doi.org/10.1007/s00027-014-0340-0

Helms, J. R., Stubbins, A., Ritchie, J. D., Minor, E. C., Kieber, D. J., & Mopper, K. (2008). Absorption spectral slopes and slope ratios as indicators of molecular weight, source and photobleaching of chromophoric dissolved organic matter. *Limnology and Oceanography*, *53*, 955–969. https://doi.org/10.4319/lo.2008.53.3.0955

Hernes, P. J., Bergamaschi, B. A., Eckard, R. S., & Spencer, R. G. (2009). Fluorescence-based proxies for lignin in freshwater dissolved organic matter. *Journal of Geophysical Research: Biogeosciences*, *114*(G4), G00F03–G00F10.

Hur, J., Park, M. H., & Schlautman, M. (2009). Microbial transformation of dissolved leaf litter organic matter and its effects on selected organic matter operational descriptors. *Environmental Science & Technology*, *43*, 2315–2321. https://doi.org/10.1021/es802773b

Hutchins, R. H., Aukes, P., Schiff, S. L., Dittmar, T., Prairie, Y. T., & Giorgio, P. A. (2017). The optical, chemical, and molecular dissolved organic matter succession along a boreal soil-stream-river continuum. *Journal of Geophysical Research: Biogeosciences*, *122*, 2892–2908. https://doi.org/10.1002/2017JG004094

IPCC. (2013). Intergovernmental Panel on Climate Change. Summary for policymakers: Climate change 2013–the physical science basis. In T. F. Stocker, D. Quin, G. Plattner, M. Tignor, S. Allen, J. Boschung, … P. Midgley (Eds.), *Working Group 1 contribution to the IPCC fifth assessment report of the Intergovernmental Panel on Climate Change* (pp. 1–27). New York, NY: Cambridge University Press

Ishii, S. K., & Boyer, T. H. (2012). Behavior of reoccurring PARAFAC components in fluorescent dissolved organic matter in natural and engineered systems: A critical review. *Environmental Science & Technology*, *46*, 2006–2017. https://doi.org/10.1021/es2043504

Jaffé, R., McKnight, D., Maie, N., Cory, R., McDowell, W. H., & Campbell, J. L. (2008). Spatial and temporal variations in DOM composition in ecosystems: The importance of long-term monitoring of optical properties. *Journal of Geophysical Research: Biogeosciences*, *113*, G04032. https://doi.org/10.1029/2008JG000683

Kaiser, K., & Kalbitz, K. (2012). Cycling downwards–dissolved organic matter in soils. *Soil Biology & Biochemistry*, *52*, 29–32. https://doi.org/10.1016/j.soilbio.2012.04.002

Kalbitz, K., Schmerwitz, J., Schwesig, D., & Matzner, E. (2003). Biodegradation of soil-derived dissolved organic matter as related to its properties. *Geoderma*, *113*, 273–291. https://doi.org/10.1016/S0016-7061(02)00365-8

Kellerman, A. M., Kothawala, D. N., Dittmar, T., & Tranvik, L. J. (2015). Persistence of dissolved organic matter in lakes related to its molecular characteristics. *Nature Geoscience*, *8*, 454. https://doi.org/10.1038/ngeo2440

Koponen, H. T., Jaakkola, T., Keinänen-Toivola, M. M., Kaipainen, S., Tuomainen, J., Servomaa, K., & Martikainen, P. J. (2006). Microbial communities, biomass, and activities in soils as affected by freeze thaw cycles. *Soil Biology and Biochemistry*, *38*, 1861–1871. https://doi.org/10.1016/j.soilbio.2005.12.010

Li, P., Lee, S. H., Lee, S. H., Lee, J. B., Lee, Y. K., Shin, H. S., & Hur, J. (2016). Seasonal and storm-driven changes in chemical composition

of dissolved organic matter: A case study of a reservoir and its forested tributaries. *Environmental Science and Pollution Research*, *23*, 24834–24845. https://doi.org/10.1007/s11356-016-7720-z

Maie, N., Scully, N. M., Pisani, O., & Jaffé, R. (2007). Composition of a protein-like fluorophore of dissolved organic matter in coastal wetland and estuarine ecosystems. *Water Research*, *41*, 563–570. https://doi.org/10.1016/j.watres.2006.11.006

Marín-Spiotta, E., Gruley, K. E., Crawford, J., Atkinson, E. E., Miesel, J. R., Greene, S., … Spencer, R. G. M. (2014). Paradigm shifts in soil organic matter research affect interpretations of aquatic carbon cycling: Transcending disciplinary and ecosystem boundaries. *Biogeochemistry*, *117*, 279–297. https://doi.org/10.1007/s10533-013-9949-7

Masiokas, M. H., Villalba, R., Luckman, B. H., Lascano, M. E., Delgado, S., & Stepanek, P. (2008). 20th-century glacier recession and regional hydroclimatic changes in northwestern Patagonia. *Global and Planetary Change*, *60*, 85–100. https://doi.org/10.1016/j.gloplacha.2006.07.031

Massana, R., Gasol, J. M., Bjørnsen, P. K., Blackburn, N., Hagstrøm, Å., Hietanen, S., … Alió, C. (1997). Measurement of bacterial size via image analysis of epifluorescence preparations: Description of an inexpensive system and solutions to some of the most common problems. *Scientia Marina*, *61*, 397–407.

Michel, K., Matzner, E., Dignac, M. F., & Kögel-Knabner, I. (2006). Properties of dissolved organic matter related to soil organic matter quality and nitrogen additions in Norway spruce forest floors. *Geoderma*, *130*, 250–264. https://doi.org/10.1016/j.geoderma.2005.01.023

Murphy, K. R., Stedmon, C. A., Graeber, D., & Bro, R. (2013). Fluorescence spectroscopy and multi-way techniques. PARAFAC. *Analytical Methods*, *5*, 6557–6566. https://doi.org/10.1039/c3ay41160e

Murphy, K. R., Stedmon, C. A., Wenig, P., & Bro, R. (2014). OpenFluor - An online spectral library of auto-fluorescence by organic compounds in the environment. *Analytical Methods*, *6*, 658–661. https://doi.org/10.1039/C3AY41935E

Norland, S. (1993). The relationship between biomass and volume of bacteria. In P. Kemp, B. F. Sherr, & J. Cole (Eds.), *Handbook of methods in aquatic microbial ecology* (pp. 303–307). Boca Raton, FL: Lewis.

Ohno, T. (2002). Fluorescence inner-filtering correction for determining the humification index of dissolved organic matter. *Environmental Science & Technology*, *36*, 742–746. https://doi.org/10.1021/es0155276

Paruelo, J. M., Beltrán, A., Jobággy, E., Sala, O. E., & Golluscio, R. A. (1998). The climate of Patagonia: General patterns and controls on biotic processes. *Ecología Austral*, *8*, 85–101.

Porter, K. G., & Feig, Y. S. (1980). The use of DAPI for identifying and counting aquatic microfloral. *Limnology and Oceanography*, *25*, 943–948. https://doi.org/10.4319/lo.1980.25.5.0943

Queimaliños, C. P., Reissig, R., Diéguez, M. C., Arcagni, M., Ribeiro Guevara, S., Campbell, L., … Arribére, M. (2012). Influence of precipitation, landscape and hydrogeomorphic lake features on pelagic allochthonous indicators in two connected ultraoligotrophic lakes of North Patagonia. *Science of the Total Environment*, *427–428*, 219–228. https://doi.org/10.1016/j.scitotenv.2012.03.085

Simon, M., & Azam, F. (1989). Protein content and protein synthesis rates of planktonic marine bacteria. *Marine Ecology Progress Series*, *51*, 201–213. https://doi.org/10.3354/meps051201

Sobczak, W. V., & Raymond, P. A. (2015). Watershed hydrology and dissolved organic matter export across time scales: Minute to millennium. *Freshwater Science*, *34*, 392–398. https://doi.org/10.1086/679747

Soto Cárdenas, C., Gerea, M., Garcia, P. E., Pérez, G. L., Diéguez, M. C., Rapacioli, R., … Queimaliños, C. (2017). Interplay between climate and hydrogeomorphic features and their effect on the seasonal variation of dissolved organic matter in shallow temperate lakes of the Southern Andes (Patagonia, Argentina): A field study based on optical properties. *Ecohydrology*, *10*,E1872. https://doi.org/10.1002/eco.1872

Spencer, R. G. M., Aiken, G. R., Butler, K. D., Dornblaser, M. M., Striegl, R. G., & Hernes, P. J. (2009). Utilizing chromophoric dissolved organic matter measurements to derive export and reactivity of dissolved organic carbon to the Arctic Ocean: A case study of the Yukon River, Alaska. *Geophysical Research Letters*, *36*, L06401.

Spencer, R. G. M., Hernes, P. J., Ruf, R., Baker, A., Dyda, R. Y., Stubbins, A., & Six, J. (2010). Temporal controls on dissolved organic matter and lignin biogeochemistry in a pristine tropical river, Democratic Republic of Congo. *Journal of Geophysical Research*, *115*, G03013.

Stedmon, C. A., & Bro, R. (2008). Characterizing dissolved organic matter fluorescence with parallel factor analysis: A tutorial. *Limnology and Oceanography, Methods*, *6*, 572–579. https://doi.org/10.4319/lom.2008.6.572

Stedmon, C. A., & Cory, R. M. (2014). Biological origins and fate of fluorescent dissolved organic matter in aquatic environments. In P. Coble, J. Lead, A. Baker, D. Reynolds, & R. Spencer (Eds.), *Aquatic organic matter fluorescence* (pp. 278–299). New York, NY: Cambridge University Press. https://doi.org/10.1017/CBO9781139045452

Stubbins, A., Spencer, R. G. M., Chen, H., Hatcher, P. G., Mopper, K., Hernes, P. J., … Six, J. (2010). Illuminated darkness: Molecular signatures of Congo River dissolved organic matter and its photochemical alteration as revealed by ultrahigh precision mass spectrometry. *Limnology and Oceanography*, *55*, 1467–1477. https://doi.org/10.4319/lo.2010.55.4.1467

Uselman, S. M., Qualls, R. G., & Lilienfein, J. (2012). Quality of soluble organic C, N, and P produced by different types and species of litter: Root litter versus leaf litter. *Soil Biology & Biochemistry*, *54*, 57–67. https://doi.org/10.1016/j.soilbio.2012.03.021

Villalba, R., Boninsegna, J. A., Veblen, T. T., Schmelter, A., & Rubulis, S. (1997). Recent trends in tree-ring records from high elevation sites in the Andes of northern Patagonia. In H. Diaz, M. Beniston, & R. Bradley (Eds.), *Climatic change at high elevation sites* (pp. 193–222). Dordrecht, The Netherlands: Springer. https://doi.org/10.1007/978-94-015-8905-5

Villalba, R., Lara, A., Masiokas, M. H., Urrutia, R., Luckman, B. H., Marshall, G. J., & Allen, K. (2012). Unusual Southern Hemisphere tree growth patterns induced by changes in the Southern Annular Mode. *Nature Geoscience*, *5*, 793–798. https://doi.org/10.1038/ngeo1613

Wetzel, R. G. (2001). *Limnology: Lake and river ecosystems*. Oxford, UK: Gulf Professional Publishing.

Yamashita, Y., & Tanoue, E. (2008). Production of bio-refractory fluorescent dissolved organic matter in the ocean interior. *Nature Geoscience*, *1*, 579. https://doi.org/10.1038/ngeo279

Zagarese, H. E., Diaz, M., Pedrozo, F., Ferraro, M., Cravero, W., & Tartarotti, B. (2001). Photodegradation of natural organic matter exposed to fluctuating levels of solar radiation. *Journal of Photochemistry and Photobiology*, *61*, 35–45. https://doi.org/10.1016/S1011-1344(01)00142-7

Zagarese, H. E., Ferraro, M., Queimaliños, C. P., Diéguez, M. C., Suárez, D. A., & Llames, M. E. (2017). Patterns of dissolved organic matter across the Patagonian landscape: A broad-scale survey of Chilean and Argentine lakes. *Marine and Freshwater Research*, *68*, 1–11.

SUPPORTING INFORMATION

Additional Supporting Information may be found online in the supporting information tab for this article.

How to cite this article: Garcia RD, Diéguez MDC, Gerea M, Garcia PE, Reissig M. Characterisation and reactivity continuum of dissolved organic matter in forested headwater catchments of Andean Patagonia. *Freshwater Biol*. 2018;00: 1–14. https://doi.org/10.1111/fwb.13114